

Kinetics and Reaction Mechanisms of Complexes with Cobalt–Carbon σ Bonds of the Type $\{(\text{NH}_3)_5\text{Co}-\text{R}\}^{n+}$ in Aqueous Solutions, a Pulse Radiolysis Study

Nurit Shaham,^[a] Alexandra Masarwa,^[a] Yoseph Matana,^[b] Haim Cohen,^[a,b] and Dan Meyerstein*^[a,c]

Keywords: Cobalt / Kinetics / N ligands / Reaction mechanisms / Radiolysis

The kinetics of formation of complexes with cobalt–carbon σ bonds in the reaction between $\{\text{Co}^{\text{II}}(\text{NH}_3)_5\text{H}_2\text{O}\}^{2+}$ or $\{\text{Co}^{\text{II}}(\text{NH}_3)_6\}^{2+}$ with different aliphatic radicals was studied in aqueous solutions using the pulse radiolysis technique. The formation of the complexes $\{(\text{NH}_3)_5\text{Co}^{\text{III}}-\text{R}\}^{n+}$ obey pseudo first order rate laws and the rate constants for $\text{R} = \text{CH}_3$ and CH_2CO_2^- are $(3.0 \pm 0.3) \times 10^7$ and $(2.1 \pm 0.3) \times 10^7 \text{ M}^{-1}\text{s}^{-1}$, re-

spectively. The UV/Vis spectra of the complexes are reported and found to be in agreement with previous results for analogous complexes. The results point out that the reactions $(\text{NH}_3)_5\text{Co}^{\text{III}}-\text{R} + \text{R}' + \text{NH}_3 \rightarrow \text{Co}(\text{NH}_3)_6^{2+} + \text{R}_2$ are fast thus limiting the radical route as a synthetic tool for the $(\text{NH}_3)_5\text{Co}^{\text{III}}-\text{R}$ complexes.

Introduction

The properties of complexes with cobalt–carbon σ bonds were widely studied for two main reasons:

1. The importance of the coenzyme vitamin B₁₂.
2. The kinetic stability of the cobalt–carbon σ bond, which provides the ability to synthesize a variety of complexes of this type.

The discovery that coenzyme B₁₂ is a cobalt(III) complex containing a cobalt–carbon σ bond initiated many studies concerning the mechanisms of formation and decomposition of these bonds. It was argued that a prerequisite for the formation of a stable alkylcobalt(III) compound is an unsaturated equatorial ligand system. Thus, the complexes studied so far mainly contained ligands, which are considered coenzyme vitamin B₁₂ analogues, i.e. unsaturated ligands bound to the cobalt ion in a planar configuration as analogous to the corrins,^[1] e.g. unsaturated tetraazamacrocyclic ligands.^[2–4] These ligands stabilize the cobalt ion in three oxidation states; +1, +2 and +3. Alkylcobalt(III) compounds containing solely saturated ligands have been reported for relatively few cases,^[4–6] the ligands were mainly saturated tetraazamacrocyclic ones, these complexes have been prepared employing various synthetic methods. Meyerstein et al.^[7] studied the formation and decomposition of $(\text{nta})\text{Co}^{\text{III}}-\text{R}$ complexes formed in the reactions of $(\text{nta})\text{cobalt(II)}$ complexes with various aliphatic radicals 'R

[where nta is nitriloacetate, $\text{N}(\text{CH}_2\text{CO}_2^-)_3$], to elucidate the factors affecting the rates of cobalt–carbon bond formation. It was found that the stability of the cobalt–carbon bond towards homolytic cleavage is in the order $\text{CH}_3 > \text{CH}_2\text{OH} > \text{CH}(\text{CH}_3)\text{OH} > \text{C}(\text{CH}_3)_2\text{OH}$. The results also pointed out, that nta indeed stabilizes transient complexes of the type $\{(\text{nta})\text{Co}^{\text{III}}-\text{R}(\text{H}_2\text{O})\}^-$. The formation and decomposition mechanisms were further studied using the high-pressure technique.^[8] It was concluded that metal–carbon bond formation is very similar to ligand-exchange processes in terms of volume changes, and follows an I_d mechanism in the case of cobalt(II). Homolysis of the cobalt–carbon bond is presumably accompanied by an additional contribution due to the volume difference between the low spin $\text{LCo}^{\text{III}}-\text{R}$ complexes and the high-spin $\text{LCo}^{\text{II}}(\text{H}_2\text{O})$ complexes.^[9] Recently, Kofod et al.^[10,11] prepared several alkylcobalt(III) complexes with ammonia ligands such as $\{(\text{NH}_3)_5\text{Co}^{\text{III}}-\text{CH}_3\}^{2+}$, *trans*- $\{\text{Co}(\text{en})_2(\text{NH}_3)(\text{CH}_3)\}^{2+}$ and $\{\text{Co}(\text{NH}_3)_6\}$ -*mer,trans*- $\{\text{Co}(\text{NO}_2)_3(\text{NH}_3)_2(\text{CH}_3)\}_2$ -*trans*- $\{\text{Co}(\text{NO}_2)_4(\text{NH}_3)_2\}$. Kofod^[10] synthesized and spectroscopically characterized the complex $\{(\text{NH}_3)_5\text{Co}^{\text{III}}-\text{CH}_3\}^{2+}$ by alkylation of $\text{Co}(\text{NH}_3)_6^{2+}$ using methylhydrazine with dioxygen as the oxidizing agent, a route that had originally been developed for the preparation of organocobalt(III) compounds with unsaturated ligands.

Basically the strength of the cobalt–carbon σ bond depends on several factors:

1. The equatorial ligands, which influence the redox potential of the central cobalt ion. Changes in the structure and identity of the ligands cause changes in the properties of the complexes. The redox potential of the central cobalt ion is affected by the σ donor character of the ligands.

^[a] Department of Chemistry, Ben-Gurion University of the Negev, Beer-Sheva, Israel

^[b] Nuclear Research Centre Negev, Beer-Sheva, Israel

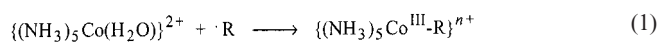
^[c] The College of Judea and Samaria, Ariel, Israel

2. The character of the ligand in the *trans* position to the R group. It was shown that for a series of cobalt–methyl compounds ligands in the *trans* position [e.g.: CN^- , NO_2^- , H_2O , NH_3 and en (1,2-ethanediamine)], considerably affect the cobalt–carbon bond length and the UV/Vis absorption spectra (in agreement with the spectroscopic series $\text{H}_2\text{O} < \text{NH}_3 < \text{CN}^- \approx \text{NO}_2^-$).^[12]

3. The character of the substituents on the aliphatic residue, R.

4. Steric hindrance which stems from the equatorial ligand structure and from the substituents on R.

It was decided to check whether the complexes $\{(\text{NH}_3)_5\text{Co}^{\text{III}}-\text{R}\}^{n+}$ can be synthesized according to Equation (1). This would open up the possibility of synthesizing a large variety of these complexes using radiation chemistry techniques. The results indicate that this technique might indeed be used, though it has its limitations. The new complexes were characterized spectrophotometrically, and their kinetics of formation and decomposition were studied.



Results

N_2O -saturated aqueous solutions containing $(0.2\text{--}4.0) \times 10^{-3}$ M CoSO_4 , 20% NH_3 and in addition 1 M of one of the following substances, CH_3OH , CH_3COONa or $(\text{CH}_3)_2\text{SO}$, were irradiated by a short electron pulse from the linear accelerator. The experimental results, see below, point out, that under these conditions the primary radicals are transformed into the desired aliphatic radicals during the pulse. As the reaction of the $\cdot\text{OH}$ radicals with NH_3 under our experimental conditions (ca. 11 M NH_3), competes with the reaction of $\cdot\text{OH}$ radicals with CH_3CO_2^- and CH_3OH ,^[13] see Table 1, the results (*vide infra*) indicate that the produced $\cdot\text{NH}_2$ radicals react with the organic substrates to produce the desired aliphatic radicals by analogous reactions to those of the $\cdot\text{OH}$ radical. This result is not surprising as the dissociation energy of the $\text{H}_2\text{N}-\text{H}$ bond is considerably larger than that of the $\text{C}-\text{H}$ bonds in CH_3CO_2^- and CH_3OH .^[14]

Table 1. Rate constants relevant to this study

Reaction	k [$\text{M}^{-1}\text{s}^{-1}$]
$(\text{CH}_3)_2\text{SO} + \cdot\text{OH} \rightarrow (\text{CH}_3)_2\text{S}(\text{O})\text{OH}$	6.6×10^9 [21]
followed by:	
$(\text{CH}_3)_2\text{S}(\text{O})\text{OH} \rightarrow \cdot\text{CH}_3 + (\text{CH}_3)\text{S}(\text{O})\text{OH}$	1.5×10^7 [s^{-1}] [21]
$(\text{CH}_3)_2\text{SO} + \cdot\text{H} \rightarrow (\text{CH}_3)_2\text{S}(\text{OH})\cdot$	2.7×10^6 [22]
$(\text{CH}_3)_2\text{SO} + e_{\text{aq}}^- \rightarrow \text{products}$	1.6×10^6 [23]
$\text{CH}_3\text{COO}^- + \cdot\text{OH} \rightarrow \cdot\text{CH}_2\text{COO}^- + \text{H}_2\text{O}$	8.5×10^7 [24]
$\text{CH}_3\text{COO}^- + \cdot\text{H} \rightarrow \cdot\text{CH}_2\text{COO}^- + \text{H}_2$	3.5×10^5 [25]
$\text{CH}_3\text{COO}^- + e_{\text{aq}}^- \rightarrow \text{products}$	$< 1.0 \times 10^6$ [26]
$\text{CH}_3\text{OH} + \cdot\text{OH} \rightarrow \cdot\text{CH}_2\text{OH} + \text{H}_2\text{O}$	9.7×10^8 [13]
$\text{CH}_3\text{OH} + \cdot\text{H} \rightarrow \cdot\text{CH}_2\text{OH} + \text{H}_2$	2.6×10^6 [13]
$\text{CH}_3\text{OH} + e_{\text{aq}}^- \rightarrow \text{products}$	$< 1.0 \times 10^4$ [13]
$\text{NH}_3 + \cdot\text{OH} \rightarrow \cdot\text{NH}_2 + \text{H}_2\text{O}$	1.0×10^8 [13]

In all the systems studied a formation reaction was observed after the formation of the aliphatic radicals (Figure 1). The formation of the intermediates (for methyl and acetate) obey pseudo-first-order rate laws (Figure 1). The observed rates are proportional to the initial concentration of $\{(\text{NH}_3)_5\text{Co}(\text{H}_2\text{O})\}^{2+}$ or $\{(\text{NH}_3)_5\text{Co}(\text{H}_2\text{O})\}^{2+}$ (Figure 2). The rates are independent of the concentration of all other components of the solution, pulse intensity and the wavelength at which the reaction is observed. The products are unstable, *vide infra*, i.e. they are not $(\text{NH}_3)_5\text{Co}(\text{H}_2\text{O})^{2+}$ or $\text{Co}(\text{NH}_3)_6^{3+}$. Therefore it is reasonable to propose that the intermediates formed in this process are of the type $\{(\text{NH}_3)_5\text{Co}^{\text{III}}-\text{R}\}^{2+}$, i.e. complexes with cobalt–carbon σ bonds, and that the reactions observed are as described in Equation (1). The results are summed up in Table 2. Though the straight lines in Figure 2 have no positive intercept, i.e. the reactions $\text{R}\cdot + \text{R}\cdot \rightarrow \text{R}_2$ do not compete with Equation (1) under the experimental conditions, the yield of the intermediates $(\text{NH}_3)_5\text{Co}^{\text{III}}-\text{R}$, as measured by its absorption, increases with an increase in $\{[(\text{NH}_3)_5\text{Co}(\text{H}_2\text{O})]^{2+}\}$ (Figure 3). The spectra of the intermediates formed, Table 3, are similar to those of other complexes of this type,^[10] a typical spectrum is shown in Figure 4.

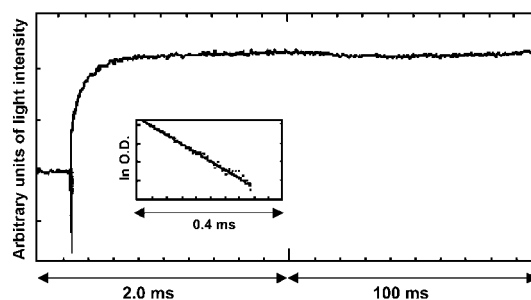


Figure 1. Formation kinetics of $\{(\text{NH}_3)_5\text{Co}^{\text{III}}-\text{CH}_2\text{CO}_2^-\}^+$; computer output of light intensity vs. time; N_2O -saturated solution with 1 M $\text{CH}_3\text{CO}_2\text{Na}$, 1×10^{-3} M CoSO_4 , ca. 20% NH_3 , the solution was irradiated with a maximum pulse and the kinetics were followed at 300 nm

Table 2. Measured rates of reaction of aliphatic radicals with $\{(\text{NH}_3)_5\text{Co}(\text{H}_2\text{O})\}^{2+}$

Reaction	$k_{1\text{meas}}$ [$\text{M}^{-1}\text{s}^{-1}$] ^[a]
$\{(\text{NH}_3)_5\text{Co}(\text{H}_2\text{O})\}^{2+} + \cdot\text{CH}_3 \rightarrow$	3.4×10^7
$\{(\text{NH}_3)_5\text{Co}-\text{CH}_3\}^{2+}$	
$\{(\text{NH}_3)_5\text{Co}(\text{H}_2\text{O})\}^{2+} + \cdot\text{CH}_2\text{COO}^- \rightarrow$	2.1×10^7
$\{(\text{NH}_3)_5\text{Co}-\text{CH}_2\text{COO}^-\}^+$	
$\{(\text{NH}_3)_5\text{Co}(\text{H}_2\text{O})\}^{2+} + \cdot\text{CH}_2\text{OH} \rightarrow$	[b]
$\{(\text{NH}_3)_5\text{Co}-\text{CH}_2\text{OH}\}^{2+}$	

^[a] The measured values are somewhat higher than k_1 , see discussion. ^[b] The results imply that this process is an equilibrium process with a very small equilibrium constant, therefore it is difficult to establish this rate constant.

Mechanism of Decomposition of the Complexes

$\{(\text{NH}_3)_5\text{Co}^{\text{III}}-\text{R}\}^{n+}$

The decomposition processes for all the intermediates in this study obey first-order rate laws. The measured decom-

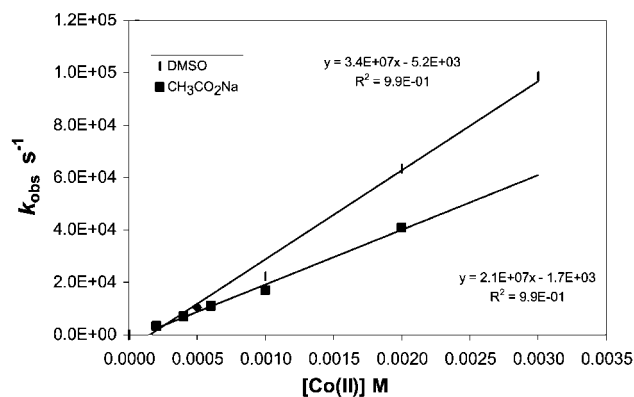


Figure 2. Dependence of the rate of formation of $\{(\text{NH}_3)_5\text{Co}-\text{CH}_3\}^{2+}$ and of $\{(\text{NH}_3)_5\text{Co}-\text{CH}_2\text{CO}_2^-\}^+$ on $\{(\text{NH}_3)_5\text{Co}(\text{H}_2\text{O})\}^{2+}$; solution composition: N_2O saturated, $(0.2-4.0)\times 10^{-3}$ M CoSO_4 , ca. 20% NH_3 and 1.0 M DMSO or $\text{CH}_3\text{CO}_2\text{Na}$

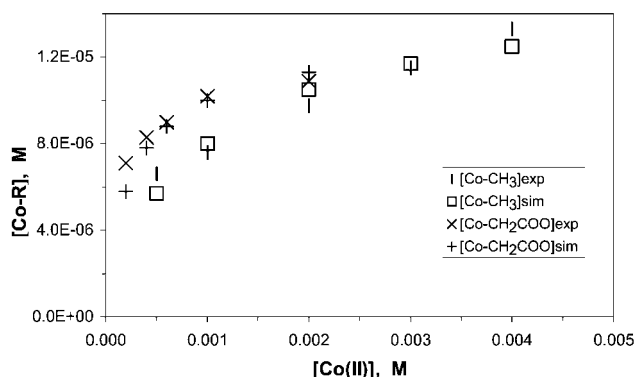


Figure 3. Dependence of $\{(\text{NH}_3)_5\text{Co}-\text{CH}_3\}^{2+}$ and $\{(\text{NH}_3)_5\text{Co}-\text{CH}_2\text{COO}^-\}^+$ on $\{(\text{NH}_3)_5\text{Co}(\text{H}_2\text{O})\}^{2+}$; experimental and simulated data; solution composition: N_2O saturated, $(0.5-4.0)\times 10^{-3}$ M CoSO_4 , ca. 20% NH_3 and 1.0 M DMSO or 1 M $\text{CH}_3\text{CO}_2\text{Na}$; measured at 350 and 300 nm, respectively, and simulated with 1.6×10^{-5} and 1.3×10^{-5} m/pulse dose rates

Table 3. UV/Vis absorption maxima of the intermediates of the type $\{(\text{NH}_3)_5\text{Co}-\text{R}\}^{n+}$

Intermediate	λ_{max} [nm]	ϵ_{max} [$\text{M}^{-1}\text{cm}^{-1}$]
$\{(\text{NH}_3)_5\text{Co}-\text{CH}_3\}^{2+}$	362, 494	183, 50
$\{(\text{NH}_3)_5\text{Co}-\text{CH}_2\text{COO}^-\}^+$	370, 505	82, 50
$\{(\text{NH}_3)_5\text{Co}-\text{CH}_2\text{OH}\}^{2+}$	330	175 ^[a]

^[a] Assuming that all the radicals react to yield the intermediate.

position rate constants (samples irradiated in a ^{60}Co γ -source) are summed up in Table 4 [as the equilibrium constant for the formation of $\{(\text{NH}_3)_5\text{Co}^{\text{III}}-\text{CH}_2\text{OH}\}^{2+}$ is small, the observed decomposition is due to the reaction between two CH_2OH radicals ($k = 1.5\times 10^9 \text{ M}^{-1}\text{s}^{-1}$)^[15]]. The final products of the decomposition reaction of the intermediate $\{(\text{NH}_3)_5\text{Co}-\text{CH}_3\}^{2+}$ were analyzed using GC and were found to be mainly ethane and methane. The ratios between ethane and methane formed were measured

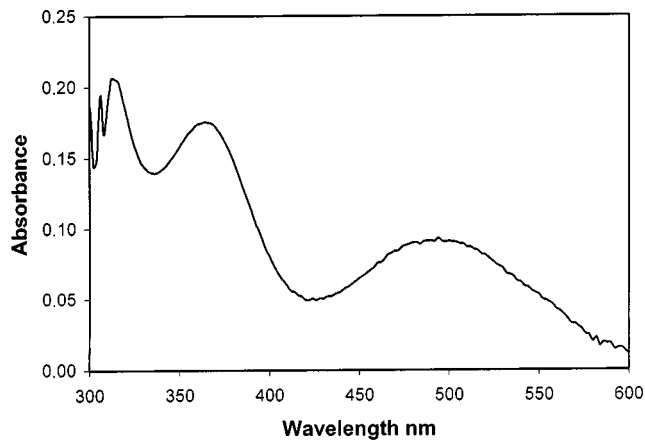


Figure 4. Spectrum of the intermediate $\{(\text{NH}_3)_5\text{Co}-\text{CH}_3\}^{2+}$; experimental conditions: N_2O saturated, 1×10^{-3} M CoSO_4 , ca. 20% NH_3 and 1.00 M DMSO, the solution was irradiated for 15 min in the ^{60}Co source

Table 4. Measured decomposition rate constants of the complexes $\{(\text{NH}_3)_5\text{Co}-\text{R}\}^{n+}$

Complex	k [s^{-1}]
$\{(\text{NH}_3)_5\text{Co}-\text{CH}_3\}^{2+}$	2.2×10^{-4}
$\{(\text{NH}_3)_5\text{Co}-\text{CH}_2\text{COO}^-\}^+$	5.3×10^{-4}

and were found to decrease with the increase of the initial $\{(\text{NH}_3)_5\text{Co}(\text{H}_2\text{O})\}^{2+}$ concentration, and increase with the number of pulses delivered to the sample, Table 5.

Table 5. Relative yields of C_2H_6 and CH_4 formed in the $(\text{CH}_3)_2\text{SO}$ system; solution composition: N_2O saturated, ca. 20% NH_3 and 1.00 M DMSO; samples were irradiated by consecutive pulses in the linear accelerator

$[\text{Co}^{2+}]$ [M]	No. of pulses	Ethane/methane ^[a] (experimental)	Ethane/methane (simulation)
4.0×10^{-4}	10	3.6	4.7
6.0×10^{-4}	10	3.0	3.2
1.0×10^{-3}	10	2.3	2.0
2.0×10^{-3}	10	1.5	1.05
1.0×10^{-3}	6	1.54	1.35
1.0×10^{-3}	4	1.50	1.05

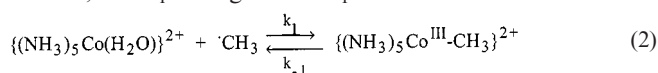
^[a] The pulses were given before the decomposition reaction occurs.

Discussion

Formation and Decomposition of the Complex $\{(\text{NH}_3)_5\text{Co}-\text{CH}_3\}^{2+}$

The experimental results indicate:

1) The reaction of the $\cdot\text{CH}_3$ radical with the cobalt complex is relatively fast and the kinetics follows a pseudo-first-order rate law. The intercept of the line in Figure 2 is close to zero, i.e. K_1 is large and k_{-1} is small.



2) However, surprisingly the yield of the intermediate formed also depends on the initial cobalt complex concentration, Figure 3.

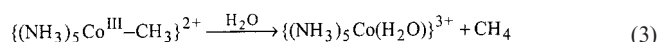
3) The decomposition reaction of the complex $\{(\text{NH}_3)_5\text{Co}^{\text{III}}-\text{CH}_3\}^{2+}$ obeys a first-order rate law, with a rate that does not depend on the concentrations of the solution components, i.e. the decomposition reaction does not proceed by homolysis.

4) The major final product is ethane, which is surprising for a first-order decomposition of the intermediate. The ratio of [ethane]/[methane] formed depends on the initial $[\text{Co}(\text{NH}_3)_6^{2+}]$ and the total number of pulses delivered to the sample, Table 5.

These results seemed to suggest that the ethane is not a product of the decomposition of the intermediate complex, $\{(\text{NH}_3)_5\text{Co}^{\text{III}}-\text{CH}_3\}^{2+}$, which decomposes heterolytically according to Equation (3). The ethane might alternatively be formed by Equation (4), however the small intercept in Figure 2 rules out that this is the major source of ethane, and suggests that Equation (5) also occurs. Reactions analogous to Equation (5) were observed for a variety of complexes, Table 6. If the rate constant of Equation (5) is high enough it will compete with Equation (2), thus explaining qualitatively the dependence of the $[\text{C}_2\text{H}_6]/[\text{CH}_4]$ ratio on the $[\text{Co}(\text{NH}_3)_6^{2+}]_0$ concentration and on the number of pulses delivered to the solution, Table 5.

Table 6. Rates of reaction of methyl radicals with $\{\text{LM}-\text{CH}_3\}^{n+}$

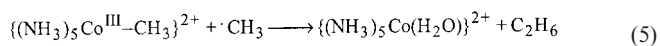
Reaction	$2k$ [$\text{M}^{-1}\text{s}^{-1}$]	Ref.
$\{(\text{NH}_3)_5\text{Co}-\text{CH}_3\}^{2+} + \cdot\text{CH}_3$	$(6 \pm 3) \times 10^8$	this work
$\{(\text{nta})(\text{H}_2\text{O})\text{Co}-\text{CH}_3\}^- + \cdot\text{CH}_3$	$(7.5 \pm 2.0) \times 10^7$	[27]
$\{(\text{nta})(\text{H}_2\text{O})\text{Fe}-\text{CH}_3\}^- + \cdot\text{CH}_3$	$(1.1 \pm 0.3) \times 10^9$	[28]
$\{(\text{nta})(\text{H}_2\text{O})\text{Mn}-\text{CH}_3\}^- + \cdot\text{CH}_3$	$(3.2 \pm 0.6) \times 10^9$	[28]
$\{(\text{cyclam})(\text{H}_2\text{O})\text{Ni}-\text{CH}_3\}^{2+} + \cdot\text{CH}_3$	8×10^7	[27]
$\{(\text{hedta})\text{Fe}-\text{CH}_3\}^{2+} + \cdot\text{CH}_3$	$(2.7 \pm 0.2) \times 10^7$	[9]



$$k = 2.2 \times 10^{-4} \text{ s}^{-1}$$



$$k = 1.6 \times 10^9 \text{ M}^{-1}\text{s}^{-1} \quad [16]$$



To check whether the addition of Equation (5) to the reaction scheme indeed explains the experimental results and in order to estimate the rate constant of this reaction, the dependence of the ratio $[\text{C}_2\text{H}_6]/[\text{CH}_4]$ was simulated. The simulation experiment was done using the pro-K global analysis/simulation software (Applied Photophysics). The simulation was run assuming that only Equations (2), (4) and (5) have to be included, since Equation (3) is relatively very slow, and assuming that the concentration of methane

formed equals the final concentration of the intermediate complex $\{(\text{NH}_3)_5\text{Co}-\text{CH}_3\}^{2+}$. The simulation had to account for the dependence of the $[\text{C}_2\text{H}_6]/[\text{CH}_4]$ ratio in the products on the $[\text{Co}(\text{NH}_3)_6^{2+}]_0$ concentration and on the number of consecutive pulses delivered to the sample, Table 5. The results clearly indicate that methane is mainly formed during the first pulses, while Equation (5) dominates during later pulses and ethane is primarily formed, Table 5. Initially the measured $k_1 = 3.4 \times 10^7 \text{ M}^{-1}\text{s}^{-1}$ was used to obtain a first estimate for k_5 . Subsequently, the effect of the thus calculated k_5 on k_1 was examined, by simulating the rates of intermediate formation and both rates were iteratively adjusted. The following values best fit the experimental data: $k_1 = (3.0 \pm 0.3) \times 10^7 \text{ M}^{-1}\text{s}^{-1}$ and $k_5 = (6 \pm 3) \times 10^8 \text{ M}^{-1}\text{s}^{-1}$. Using these rate constants the concentrations of $\{(\text{NH}_3)_5\text{Co}-\text{CH}_3\}^{2+}$ by one pulse were calculated and the thus simulated data compared with those experimentally obtained from the optical density (O.D.) due to the transient complex, Figure 3. Obviously these rate constants simulate well with this data. The simulation points out that the yield of ethane according to Equation (4)^[16] is negligible under most experimental conditions; k_5 can be compared to other reported values for analogous reactions, see Table 6. The rate constant for Equation (5) is at the higher end of the published data for these types of reactions.

It is of interest to compare the properties of $\{(\text{nta})(\text{H}_2\text{O})\text{Co}^{\text{III}}-\text{CH}_3\}^-$ [7] and $\{(\text{NH}_3)_5\text{Co}-\text{CH}_3\}^{2+}$. The former decomposes homolytically considerably faster than the heterolytic decomposition of the latter one. This is probably due to the fact that $\{\text{Co}(\text{NH}_3)_6\}^{2+}$ is a considerably stronger reducing agent than $\{\text{Co}(\text{nta})(\text{H}_2\text{O})_2\}^-$ [17] and therefore the electrons of the metal-carbon σ bond are nearer to the cobalt center in the $\{(\text{nta})(\text{H}_2\text{O})\text{Co}^{\text{III}}-\text{CH}_3\}^-$ complex. In other words the cobalt-carbon bond in $\{(\text{NH}_3)_5\text{Co}-\text{CH}_3\}^{2+}$ has a more ionic nature than that in $\{(\text{nta})(\text{H}_2\text{O})\text{Co}^{\text{III}}-\text{CH}_3\}^-$ which is more covalent and therefore tends more towards homolysis.

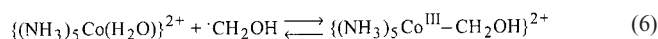
Formation and Decomposition of the Complex $\{(\text{NH}_3)_5\text{Co}-\text{CH}_2\text{CO}_2\}^+$

The acetate system behaves analogously to the methyl system. Formation and decomposition rates were measured (Tables 2 and 4) and corresponding dependencies of the formation rate constant and the intermediate concentration on initial cobalt(II) concentration were found (Figures 2 and 3). Therefore it is reasonable to conclude that the same reaction mechanism [analogous to Equations (2)–(5)] applies. The final products in this system were not measured as one of the possible products – acetate – is identical to the starting material. The rate for the reaction of the acetate radical with the intermediate (k_5 analogue) for this system was derived from a simulation of the dependency of the intermediate concentration versus the initial Co^{II} concentration (Figure 3) using the measured formation constant and a radical reaction constant (k_4 analogue) of $5.0 \times 10^8 \text{ M}^{-1}\text{s}^{-1}$.^[15] The derived rate constant for the reaction of the intermediate with the acetate radical, $k_5 = (1 \pm 0.5) \times 10^7$

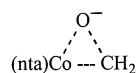
$M^{-1}s^{-1}$, is considerably lower than that for the methyl system. This observation is tentatively attributed to higher steric hindrance in this system.

Formation and Decomposition of the Complex $\{(NH_3)_5Co-CH_2OH\}^{2+}$

The formation constant of the intermediate $\{(NH_3)_5Co-CH_2OH\}^{2+}$ could not be measured as in this case the back reaction of Equation (6), the homolysis, is apparently fast.



The experimental results point out that the equilibrium constant of Equation (6) is much smaller than that measured for the analogous intermediate with nta as ligand. In the nta analog it was suggested^[7] that the intermediate formed is $\{(nta)(Co^{III}-CH_2O^-)\}$, this intermediate does not decompose readily according to the homolytic reaction since it is stabilized by partial bonding of the oxygen atom to the cobalt center due to electrostatic interactions;^[7] i.e. the intermediate formed is:



As in the NH_3 system the intermediate formed is $\{(NH_3)_5Co-CH_2OH\}^{2+}$ and no *cis* ammonia release is expected^[18] as no such stabilization is possible and it decomposes very fast according to the homolytic pathway.

Spectra of the Complexes $\{(NH_3)_5Co^{III}-R\}^{n+}$

The general spectra of the $\{(NH_3)_5Co^{III}-R\}^{n+}$ complexes resemble the spectrum of the complex $\{(NH_3)_5Co^{III}-CH_3\}^{2+}$,^[10] and the spectra of the complexes $\{(H_2O)(nta)Co^{III}-R\}^{2+}$.^[7] This confirms the identity of the nature of the transient complexes formed, as complexes of cobalt(III) with cobalt–carbon σ bonds, $\{(NH_3)_5Co^{III}-R\}^{n+}$.

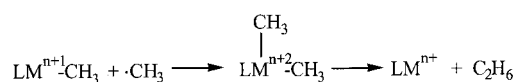
Concluding Remarks

The rate constants measured in this study, for the formation of the cobalt complexes with the cobalt–carbon σ bonds, with the different radicals, are similar to the known rate constants for ligand exchange of the complex $\{Co(H_2O)_6\}^{2+}$ in aqueous solutions, $k = 5 \times 10^6 s^{-1}$. Reactions leading to the formation of the metal–carbon bonds clearly proceed according to the inner-sphere mechanism. The results are thus in agreement with a mechanism where the rate-determining step is the ligand-exchange step. Similar conclusions were reported previously for a variety of reactions in which metal–carbon σ bonds are formed by radical reactions.^[2,7,19]

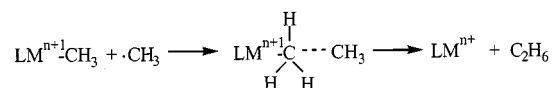
A comparison of the rates of reaction of $\cdot CH_3$ radicals with a variety of complexes of the type $L_mM^{n+1}-CH_3$, Table 6, is of interest. Though all the other reactions measured are for $L_mM^{n+1}-CH_3$ complexes which decompose homolytically, the rate constant for $\{(NH_3)_5Co^{III}-CH_3\}^{2+}$, which decomposes heterolytically, falls well into the observed range for the other reactions, i.e. the rate constants of these reactions do not depend strongly on the “ionicity” or “covalency” of the metal–carbon σ bond. Contrary to the previously published systems, which decompose homolytically (with the exception of the copper systems, which decompose in a bimolecular reaction), $\{(NH_3)_5Co-CH_3\}^{2+}$ decomposes heterolytically, implying that the Co–CH₃ bond is considerably more ionic.

In principle two possible mechanisms might be envisioned for the radical complex reaction:

a) a second CH_3 radical coordinates at the *cis* position to the first one, followed by reductive elimination of ethane:



b) the second CH_3 radical attacks, and binds to, the carbon atom bound to the central metal cation:



Reaction a) can be disqualified, based on the velocity of the reaction, as the derived reaction rate for the process is significantly faster than typical ligand exchange reactions for such a system. Recently, van Eldik et. al.^[18] measured the ligand exchange rate for the *trans*-labilized NH_3 ligand of the $\{(NH_3)_5Co-CH_3\}^{2+}$ system as $k_{sat} = 1.8 s^{-1}$ (a *cis* ligand should be more difficult to exchange). This mechanism is also in agreement with the observation that $k_{(NH_3)_5Co^{III}-CH_3} + \cdot CH_3 \gg k_{(NH_3)_5Co^{III}-CH_2CO_2^-} + \cdot CH_2CO_2^-$ as the latter reaction is sterically hindered.

Complexes with cobalt–carbon σ bonds can be synthesized by a radical process. Nevertheless, this technique has a disadvantage, the results imply that the reaction according to Equation (5) is very fast, especially for systems without steric hindrance, in comparison to Equation (2). Therefore, the attainable yields of the desired intermediates are expected to be relatively low.

Experimental Section

Materials: All solutions were prepared from AR grade chemicals and from distilled water which was further purified by passing through a Milli Q Millipore setup, final resistivity $> 10 M\Omega/cm$.

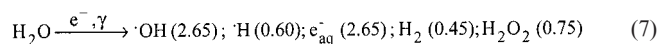
pH: The pH was measured with a Corning 22 pH meter and adjusted by addition of $HClO_4$ and/or $NaOH$.

Radiolytic Technique: Pulse radiolysis experiments were carried out using the Varian 7715 linear electron accelerator at the Hebrew

University of Jerusalem. The pulse duration was 0.1–1.5 μs with a 200-mA current of 5-MeV electrons. The dose per pulse was 3–30 Gray. Irradiations were carried out in a 4-cm spectroil optical cell, the analyzing light was passed three times through the cell. A 150-W xenon arc produced the analyzing light. The experimental setup was identical with that described earlier in detail.^[20] For dosimetry, an N_2O -saturated solution containing $1 \times 10^{-3} \text{ M Fe(CN)}_6^{4-}$ was used. The yield was measured by using $\epsilon_{420} = 1000 \text{ M}^{-1}\text{cm}^{-1}$. The values of the molar extinction coefficient calculated from the dosimetry measurements have an error limit of $\pm 15\%$ due to the scatter in the pulse intensity and due to uncertainties in G values. A ^{60}Co source, Noratom, with a dose rate of ca. 6 Gray/min was used for low-dose rate experiments and product analysis.

Product Analysis: GC analysis: 30-mL samples in closed glass vials under N_2O were irradiated by the linear accelerator and/or by the ^{60}Co source. The gaseous products were analyzed using a Varian Model 3700 gas chromatograph.

Production of Radicals: The radiolysis of water in dilute aqueous solutions can be summarized as follows:



(G values in parentheses, are defined as the number of molecules of each product/100 eV radiation absorbed by the solution).^[20] In concentrated solutions the yields of the radicals are somewhat higher and those of H_2O_2 and H_2 are somewhat lower. In N_2O -saturated solutions the hydrated electron is converted into the hydroxyl radical via:^[13]



at $\text{pH} > 3$ the contribution of $\cdot\text{H}$ atoms to the total free radical yield is less than 10%. Methyl radicals were produced by reactions summarized in Table 1. The other alkyl radicals used in this study were prepared by hydrogen abstraction reactions of the primary radicals with the appropriate aliphatic solutes, these reactions are also summarized in Table 1.

Acknowledgments

This study was supported in part by a grant from the Budgeting and Planning Committee of The Council of Higher Education and

the Israel Atomic Energy Commission. D. M. wishes to thank the Alexander von Humboldt Foundation for support and Mrs. Irene Evens for her ongoing interest and support.

- ^[1] J. Halpern, *Acc. Chem. Res.* **1982**, *15*, 238.
^[2] H. Elroi, D. Meyerstein, *J. Am. Chem. Soc.* **1978**, *100*, 5540.
^[3] J. F. Endicott, K. P. Balakrishnan, C. L. Wong, *J. Am. Chem. Soc.* **1980**, *102*, 551.
^[4] C. Y. Mok, J. F. Endicott, *J. Am. Chem. Soc.* **1978**, *100*, 123.
^[5] T. S. Roche, J. F. Endicott, *J. Am. Chem. Soc.* **1972**, *94*, 8622.
^[6] T. S. Roche, J. F. Endicott, *J. Am. Chem. Soc.* **1974**, *13*, 1575.
^[7] D. Meyerstein, H. A. Schwarz, *J. Chem. Soc., Faraday Trans. 1* **1988**, *84*, 2933–2949.
^[8] R. van Eldik, H. Cohen, D. Meyerstein, *Angew. Chem. Int. Ed. Engl.* **1991**, *30*, 1158.
^[9] S. Goldstein, G. Czapski, R. van Eldik, N. Shaham, H. Cohen, D. Meyerstein, *Inorg. Chem.*, in press.
^[10] P. Kofod, *Inorg. Chem.* **1995**, *34*, 2768.
^[11] P. Kofod, P. Harris, S. Larsen, *Inorg. Chem.* **1997**, *36*.
^[12] Y. Abe, H. Ogino, *Bull. Chem. Soc. Jpn.* **1989**, *62*, 56.
^[13] G. V. Buxton, C. L. Greenstock, W. P. Helman, A. B. Ross, *J. Phys. Chem. Ref. Data* **1988**, *17*, 513–886.
^[14] T. L. Cottrell, *The Strengths of Chemical Bonds*, 2nd ed., Butterworths, London, **1958**.
^[15] M. Simic, P. Neta, E. Hayon, *J. Phys. Chem.* **1969**, *73*, 3794.
^[16] P. Neta, J. Grodkowski, A. B. Ross, *J. Phys. Chem. Ref. Data* **1996**, *25*, 709–1050.
^[17] IUPAC Stability Constants Database, Academic Software, **1993**.
^[18] C. Ducker-Benfer, M. S. A. Hamza, C. Eckhardt, R. van Eldik, *Eur. J. Inorg. Chem.* **2000**, 1563.
^[19] R. van Eldik, H. Cohen, D. Meyerstein, *Inorg. Chem.* **1994**, *33*, 1566.
^[20] M. S. Matheson, L. M. Dorfman, *Pulse Radiolysis*; MIT press, Cambridge, **1969**.
^[21] D. Veitwisch, E. Janata, K. D. Asmus, *J. Chem. Soc., Perkin Trans. 2* **1980**, 146.
^[22] S. A. Chandhri, M. Goebel, T. Freyholdt, K. D. Asmus, *J. Am. Chem. Soc.* **1984**, *106*, 5988.
^[23] A. M. Koulkes-pujo, B. D. Michael, E. J. Hart, *J. Radiat. Phys. Chem.* **1971**, *3*, 33.
^[24] H. Cohen, D. Meyerstein, *Inorg. Chem.* **1986**, *25*, 1506.
^[25] P. Neta, G. R. Holdern, R. H. Schuler, *J. Phys. Chem.* **1971**, *75*, 449.
^[26] S. Gordon, E. J. Hart, M. S. Matheson, J. Rabani, J. K. Thomas, *Discuss. Faraday Soc.* **1963**, *36*, 193.
^[27] A. Sauer, H. Cohen, D. Meyerstein, *Inorg. Chem.* **1989**, *28*, 2511–2512.
^[28] H. Cohen, D. Meyerstein, *Inorg. Chem.* **1988**, *27*, 3429.

Received July 3, 2001
 [O01247]